IRANIAN JOURNAL OF CATALYSIS

Synthesis and characterization of Pt₃Co bimetallic nanoparticles supported on MWCNT as an electrocatalyst for methanol oxidation

Mohammad Hossein Nobahari[a], Ahmad Nozad Golikand[a,b,*], Mojtaba Bagherzadeh[c,*]

[a]Department of Chemistry, Shahr-e-Qods Branch, Islamic Azad University, Tehran, Iran.

[b]Material and Nuclear Fuel Research School, NSTRI, Tehran, Iran.

[c]Material and Nuclear Fuel Research School, NSTRI, 81465-1589, Isfahan, Iran.

ABSTRACT

The impregnation method was used to synthesize Pt and Pt₃Co supported on MWCNTs applying NaBH₄ as the reducing agent. The structure, morphology, and chemical composition of the electrocatalysts were characterized through SEM, XRD, and EDX. X-ray diffraction showed a good crystallinity of the supported Pt nanoparticles on the composites and showed the formation of Pt₃Co alloy. The SEM images revealed that the particles of Pt₃Co were deposited uniformly on the surface of MWCNT with a diameter of 10 nm. EDX analysis confirmed the surface segregation of Co and Pt occurred (1:3 surface atomic ratio Pt-Co) for the Pt₃Co/MWCNT nanocomposite. The Pt₃Co/MWCNTs and Pt/MWCNTs electrocatalysts' electrochemical performance was assessed against the methanol oxidation reaction (MOR) in 0.5 M H₂SO₄ solution using the chronoamperometry (CA) and the cyclic voltammetry (CV) methods. The minimum onset potential and the largest oxidation current density were obtained at Pt₃Co/MWCNTs electrocatalyst. The Pt₃Co/MWCNT catalyst with a good alloying degree has been shown to have better anti-poisoning ability, electrochemical activity, and long-term durability than Pt/MWCNT catalysts, approved by the bimetallic catalysts' bi-functional mechanism.

Keywords: Pt₃Co electrocatalyst, Methanol oxidation reaction, Electrochemical activity, Direct methanol fuel cells.

1. Introduction

The progression of novel materials that can overcome complicated difficulties in clean energy conversion, generation, and storage is crucial for obtaining a substitute for environmentally unfriendly fossil fuels. Fuel cells are efficient, clean and suitable for renewable energy sources and carriers needed for sustainable progression and security of energy. Recently, the methanol electro-oxidation has attracted the attention of scholars since direct methanol fuel cells (DMFCs) are great power sources for future [1-3]. As with fuel, methanol has many privileges in comparison with pure hydrogen. Methanol has a higher density of energy compared with hydrogen. It could be conveniently transported, stored, and controlled with the infrastructure as a liquid at environment conditions [4,5].

Numerous electrocatalysts have been used for oxidization of methanol [6-11], but the largest electrocatalytic activity is obtained at Pt and Pt-based alloys [12,13]. The high adsorption of carbon monoxide on Pt slows down the methanol oxidation reaction's (MOR) kinetics [14,15], assuming the high amount of Pt metal as a catalyst. Two techniques have been chosen to solve the problems. The first is based on the Pt nanoparticles' dispersion on an appropriate support. Different types of substrates have been assessed including polymer matrices [16,17], carbon nanotubes [18-20], and carbon black [21-23]. CNTs have been reported as the major focus of numerous studies, owing to their superior structural and electrical features including good electronic conductivity, great chemically active surface, and great chemical stability [24-26].

One of the 3d transition metals such as cobalt, iron, and nickel can be applied to change the Pt catalysts' nature for elevated activity [27-31]. These transition metals are less expensive compared with ruthenium.

*Corresponding author emails: anozad@aeoi.org.ir
Tel.: +98 21 88221117; Fax: +98 21 8822 1117
bagherzadeh@iaush.ac.ir; mjmo123@yahoo.com
Tel.: +98 31 3891 2082; Fax: +98 31 3891 2623

The addition of a co-catalyst to platinum can improve the electrocatalytic function of active sites via reducing problems of poisoning. One of the difficulties for determination of the impact of alloying by supported catalysts is that a supported catalyst's activity may possess a broad range of values based on its preparation method on the microstructure. The nanoparticles' inherent activity is based on shape, particle size, and composition. There is no separate value of the specific activity if they normalized by the area of Pt surface. Since the particles of alloyed Pt catalyst cannot have the similar particle size or form as Pt catalysts, a plain comparison of activity normalized through mass or surface area is not adequate to diagnose real alloying influences. Moreover, since surface segregation and segregation-triggered variations in the surface electronic features are not known for nanoparticles of Pt-bimetallic, the impact of atomic structure and chemical composition on reactivity has not been specified yet. These complications regarding supported catalysts emphasize the need for investigation of the effects of atomic structure and composition of intermetallic on MOR. Bimetallic Pt-Co catalyst shows a superior electrochemical activity compared with Pt-Ni and Pt-Fe catalyst [32,33]. Thus, this finding leads us to deeply assess the Pt-Co catalyst's electrochemical activity on CNT for application of DMFC. Here, advanced concepts can be utilized to comprehend and anticipate the MOR reactivity induced by the influences of alloying Pt with the Co in PtCo/MWCNTs electrocatalyst.

This study aimed to assess the coordination atomic between structures of binary Pt_3Co/MWCNTs nanoparticles and their manipulation to enhance the electrocatalysts provided by chemical reduction employing a strong reducing agent ($NaBH_4$). The surface was further characterized using X-ray diffraction (XRD), scanning electron microscopy (SEM), and energy dispersive X-ray spectroscopy (EDX). The electrocatalytic activity of these Pt_3Co/MWCNTs catalysts was evaluated toward MOR in H_2SO_4 solution. The result indicates that the higher Pt_3Co/MWCNTs electrocatalytic activity and platinum active sites' stability in MOR can be attributed mainly to the atomic structure and morphology of the electrocatalysts and composition of Pt_3Co nanoparticles on MWCNTs.

2. Experimental

2.1. Materials and apparatus

Cobalt chloride hexahydrate ($CoCl_2.6H_2O$), Hexachloroplatinic acid hexahydrate ($H_2PtCl_6.6H_2O$),

and sodium borohydride ($NaBH_4$) were obtained from Merck. MWCNTs were purchased from Alfa ascer and Nafion (5 w.t. %) were purchased from Aldrich. XRD analyses were done on an STOE-STADV X-ray diffractometer with the Cu Kα (k=1.5406Å) radiation source functioning at 40 kV and 40 mA. The nanocomposites' bulk composition was evaluated by energy dispersive X-ray analysis (EDX) in a SEM (MIRA3 LMU, TESCAN co.)

2.2. Preparation of electrocatalysts

Multi-wall carbon nanotubes (MWCNTs) were handled by refluxing in H_2SO_4 98% and HNO_3 70% (3:1 V/V) mixture at 90 °C. In order to prepare Pt_3Co/MWCNTs nanocomposites, 50 mg of the MWCNTs were entered into 20 ml deionized water. Then, an aqueous solution (1.3 ml, 0.05 M) of hexachloroplatinic acid hexahydrate ($H_2PtCl_6.6H_2O$) and (50 ml, 0.01 M) cobalt chloride hexahydrate ($CoCl_2.6H_2O$) were added to the suspension dropwise and were vigorously mixed. The black suspension was put in an ultrasonic bath for 30 min. The solution pH was set at 9.0 through adding an adequate amount of NaOH 1 M aqueous solution. Afterwards, sodium borohydride ($NaBH_4$) solution 20 ml was added slowly to the suspension which was treated with vigorous stirring, sonicated for 30 minutes and stored for 12 h at room temperature. The induced sample was washed by a large amount of deionized water and dried in a vacuum oven for 8 h at 70 °C. The Pt_3Co/MWCNT catalyst with a nominal atomic ratio of Pt: Co 3:1 was achieved (20 w.t% overall metal loaded).

2.3. Electrochemical activity measurement

The sample's electrocatalytic activities were estimated in a conventional three-electrode cell by an Autolab Methrom. The three-electrode cell consisted of a Pt wire serving as the counter electrode, an Ag/AgCl (3 M KCl) electrode used as the reference electrode and glassy carbon (GC) disk (3 mm in diameter) electrode with coated catalysts used as the working electrode. The working electrode was produced according to following instructions: 5 mg of catalyst powder was added into a mixed solution (200 µL of ethanol, 200 µL of water, and 50 µL of 5% Nafion 117 solution) with 30 min ultrasonication to make a uniform black suspension. 20 µL of the suspension was pipetted carefully onto the surface of GC electrode, and the coating was dried at 60°C for 20 min. The catalysts' electrochemical surface area values were determined via hydrogen absorption/desorption' cyclic voltammetry (CV) at room temperature in 0.5 M H_2SO_4 solution. The catalysts' electrocatalytic activity for oxidation of methanol was specified through collecting CVs in a 0.5 H_2SO_4 and 1 M methanol solution at several scanning

rates. Numerous activation was scanned until obtaining reproducible voltammograms. The last voltammograms (5th voltammogram) were merely employed for comparison of the specified catalysts' catalytic activity. The tests of chronoamperometry were performed for 20 min at 0.6 V. The curves of chronopotentiometry were recorded in 1 M methanol solution and 0.5 M H_2SO_4. The applied current was estimated at 0.6 V from the forward scanning of the corresponding cyclic voltammogram.

3. Results and Discussion

3.1 Characterization of electrocatalysts

Fig. 1 depicts the XRD patterns of the Pt/MWCNT and Pt_3Co/MWCNT prepared samples. For the Pt/MWCNT composite, the observed broad peak at about 2θ =26.0° can be indexed to the hexagonal graphite structure's (002) diffraction in MWCNTs. In addition, the strong peaks of diffraction at 39.5°, 46.8°, and 67.6° can be, respectively, attributed to the characteristic (111), (200), and (220) crystalline planes of Pt, characteristic of Pt fcc structure, showing the supported Pt nanoparticles' decent crystallinity in the composite (JCPD card No. 00-029-0499) [34]. In the case of the Pt_3Co/MWCNT catalyst, the peaks of Pt diffraction are modified to higher angles with respect of those of Pt catalyst. This shifting is because of the Pt lattice contraction made by the Co incorporation. For the Pt_3Co/MWCNT, there are no peaks attributed to the Co structure; this may be due to this fact that species of Co is present in amorphous form of tiny crystallites. However, based on the platinum peak (Pt (200) at 2θ of nearly 68°), the mean size of platinum crystallite was estimated to be 10.7±0.2 nm using Sherrer's equation [35,36].

The results of XRD were further proved by SEM and EDX analysis. Fig. 2 shows the Pt/MWCNT and Pt_3Co/MWCNT composite samples' SEM images, with an average particles size around 10 nm, were detected clearly. An analysis of EDX in Fig. 3 confirmed that the composite materials have Co, Pt, and C elements, and the overall metal loading value is ca. 18 w.t.%. The Pt: Co atomic ratio in the Pt_3Co/MWCNT nanoparticles was about 3:1 (Table. 1). The results confirmed the successful preparation of the Pt/MWCNT and Pt_3Co/MWCNT catalyst samples.

3.2. The electrochemical results

The Pt/MWCNT and Pt_3Co/MWCNT's electrocatalytic activity at the same catalyst mass loading was specified via CV (Fig. 4). The catalysts exhibit the peaks of H_2 desorption/adsorption in the potential range -0.2 to 1.2 V (vs. Ag/AgCl). Fig. 4 shows that both of the catalysts showed a tailed oxidation peak related to Pt oxidation to PtO reaction and a sharp peak corresponding to reduction of PtO to Pt reaction (a common voltammetric reaction of Pt surface in acidic conditions) in 500 mV. In the region of hydrogen adsorption/desorption, pure Pt demonstrate the resolved peaks related to weakly and robustly bonded species of hydrogen on various Pt crystal faces [37]. In addition, the Pt_3Co/MWCNT exhibits current peaks which are well defined and related to processes of hydrogen adsorption/desorption. According to Fig. 4, the H_2 adsorption/desorption peaks are larger for the Pt_3Co/MWCNT catalyst than those for Pt/MWCNT catalysts, indicating that the catalytic activity of Pt_3Co/MWCNT and using Pt_3Co are preferred for nanostructure catalysts compared with pure catalysts of Pt.
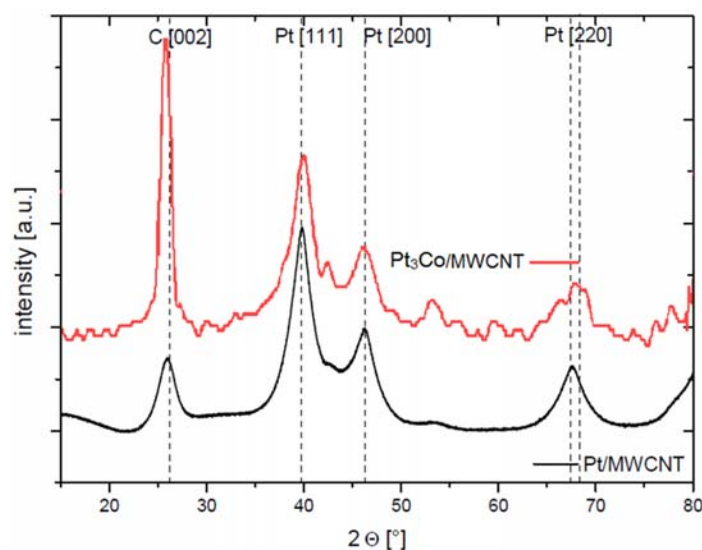

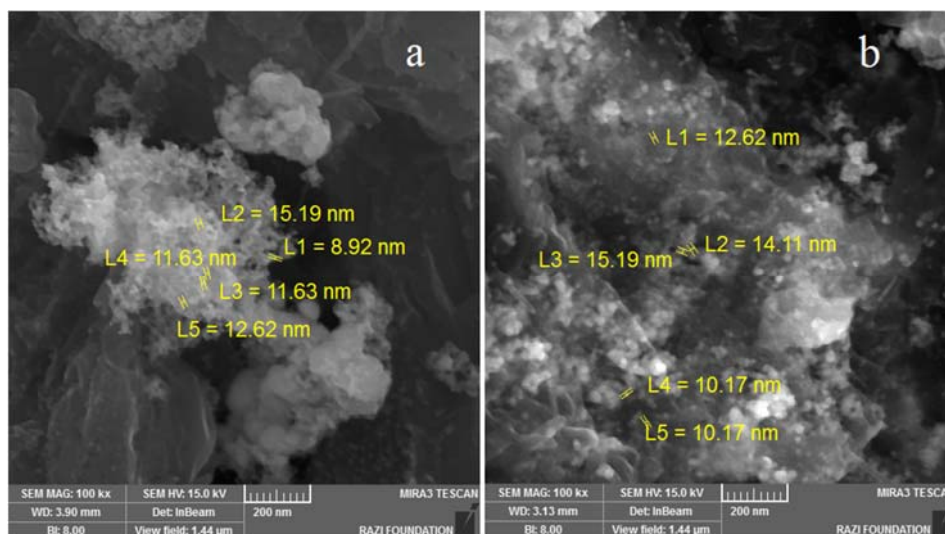**Fig. 1.** The XRD patterns of Pt/MWCNT, Pt_3Co/MWCNT samples.

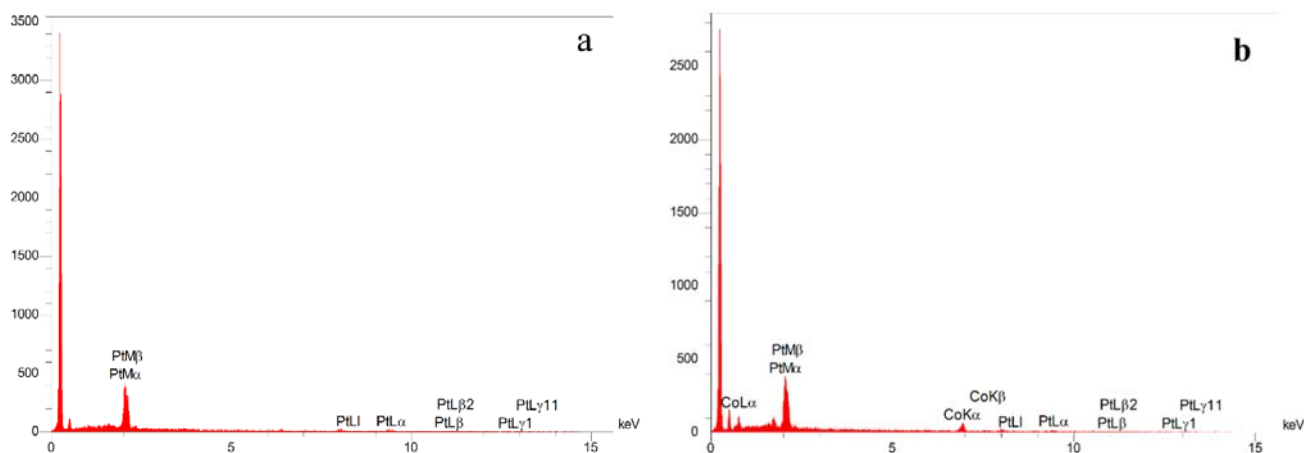**Fig. 2.** The SEM images of (a) Pt/MWCNT, and (b) Pt$_3$Co/MWCNT samples.

Fig. 3. The EDX spectrums of (a) Pt/MWCNTs, and (b) Pt$_3$Co/MWCNTs samples.

Table 1. Variation of the elemental composition of Pt/MWCNTs and Pt$_3$Co/MWCNTs electrocatalysts according to EDX analysis.

Catalyst	C		Pt		Co	
	wt.%	at.%	wt.%	at.%	wt.%	at.%
Pt/MWCNTs	81.61	98.63	18.39	1.37	-	-
Pt$_3$Co/MWCNTs	82.01	97.86	14.45	1.02	3.54	0.71

The electrocatalytic activity of Pt$_3$Co/MWCNT and Pt/MWCNT for MOR was studied via recording CVs in deaerated 0.5 M aqueous solution of H$_2$SO$_4$ containing 1 M CH$_3$OH at room temperature. Both catalysts' CVs which are normalized by the Pt mass (mass activity) are displayed in Fig. 5. The features of CV are common to methanol electro-oxidation on Pt electrode in acidic media with two anodic peaks: one peak in the reverse sweep between 0.9 and 0.6 V because of oxidative elimination of incomplete oxidized intermediates made in the forward sweep and the other in the forward sweep between 0.4 and 0.8 V which corresponds to methanol oxidation. Higher current density of forward peak shows a more rapid rate of an electrochemical reaction. The current of peak in the forward sweep for the Pt$_3$Co/MWCNT was 3.65 mA, which is higher than that for Pt/MWCNT (2.78) mA. Furthermore, the potentials of peak for reverse and forward scans changed to more anodic potentials for the Pt$_3$Co/MWCNT; This happens due to the alloying influence of Co on the electrocatalyst of Pt$_3$Co/MWCNT.
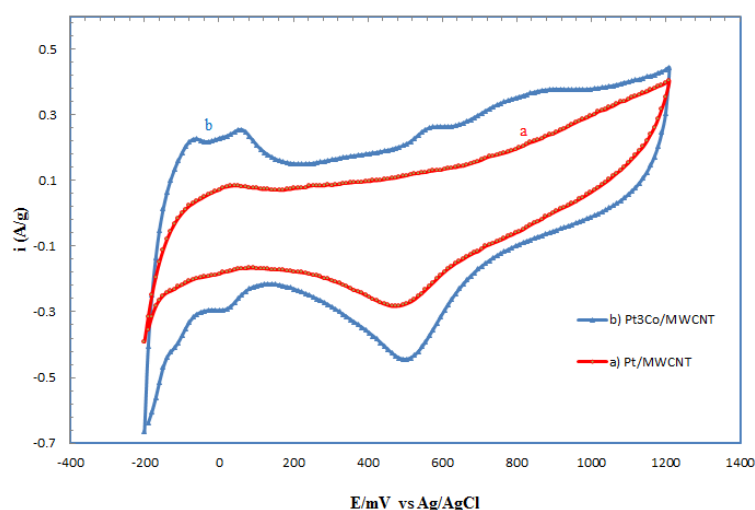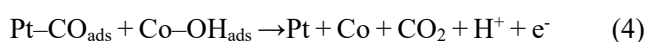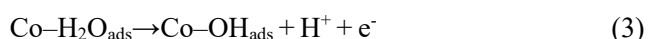
Fig. 4. The cyclic voltammograms of a) Pt/MWCNTs and b) Pt$_3$Co/MWCNTs electrocatalyst samples, in 0.5 M H$_2$SO$_4$ solution. The potential range is from −200 to +1200 mV at scan rate of 50 mV s^{-1}.

However, the higher Pt$_3$Co/MVCNT's electrocatalytic activity corresponds to more decreased state of Pt in this catalyst because of alloying with Co metal. Proposed mechanism for electrocatalytic methanol oxidation at the Pt$_3$Co/MWCNT catalyst can be explained as follows:

Generally, water splitting is a rate-determining phase in oxidation of methanol on Pt catalyst [38]. Furthermore, its reaction takes place at great potentials about 0.7 V (vs. NHE) on a surface of pure platinum [39], That is why the pure platinum is a poorer electrocatalyst for DMFCs' anodic reaction. This problem can be overcome by incorporation of the second element like Fe, Ni, and Co, to the Pt lattice [32]. The obtained matters can improve the methanol electro-oxidation reaction's overall process, recognized as a bi-functional mechanism as follows:

$$Pt + CH_3OH \rightarrow 4H^+ + Pt{-}CO_{ads} + 4e^- \qquad (1)$$

$$Co + H_2O \rightarrow Co{-}H_2O_{ads} \qquad (2)$$

$$Co{-}H_2O_{ads} \rightarrow Co{-}OH_{ads} + H^+ + e^- \qquad (3)$$

$$Pt{-}CO_{ads} + Co{-}OH_{ads} \rightarrow Pt + Co + CO_2 + H^+ + e^- \qquad (4)$$

The improved activity of Pt$_3$Co can be assigned to the mechanisms compared with pure Pt [40,41]: (1) Since cobalt is more electropositive than platinum, alloying Pt with Co can decrease the Pt electronic binding energy to place Pt in a further reduced state and develop the C–H cleavage reaction. (2) Cobalt oxide render a source of oxygen for oxidation of CO at lower capacities [24,42]. CO poisoning that came from equation (1) is the main problem in deactivation of Pt catalyst in MOR. According to the above proposed mechanism, Co can

act as an anti-poisoning agent in the catalyst also. (eq. 2-4).

For evaluating the anti-poisoning performance of an electrocatalyst in MOR, the forward anodic peak current (I_f) ratio to the reverse anodic peak current (I_b) will be examined [43]. A higher value of the I_f/I_b provides superior methanol oxidation for carbon dioxide in the forward scanning and lower electrocatalysts' poisoning through the CO-like intermediates. In Fig. 5, the I_f/I_b values of Pt$_3$Co/MWCNT and Pt/MWCNT are, respectively, 0.96 and 0.93. Although the observed enhancement is not very impressive, relative increase of I_f/I_b implies that Co metal has a positive role in enhancing the resistance of catalyst to poisoning impacts. The observed enhancement in Pt$_3$Co/MWCNT catalyst performance in comparison to the Pt/MWCNT can be explained by the bi-functional theory [44], and supporting effects [34,44] as follows:

According to the bi-functional theory, CO species adsorb on the Pt surface's active sites, whereas OH attaches to the atoms of cobalt to produce Co–OH$_{ads}$ [34,45]. This species of hydroxyl can oxidize the adsorbed CO on Pt surface, inducing a clean catalyst for more oxidation reaction (see eq. 2-4). On the other hand, the catalyst support is crucial in the electro-oxidation reaction. This is clear from the Pt catalyst's activity dependence to oxidize CO on the support nature. Multi-walled carbon nanotubes as a support for nanoparticles of Pt–Co present another explanation for their observed good electrocatalytic activity [46,47]. This results from the great number of the oxides, which include the hydroxyl and carboxylic groups on the MWCNTs' side walls.
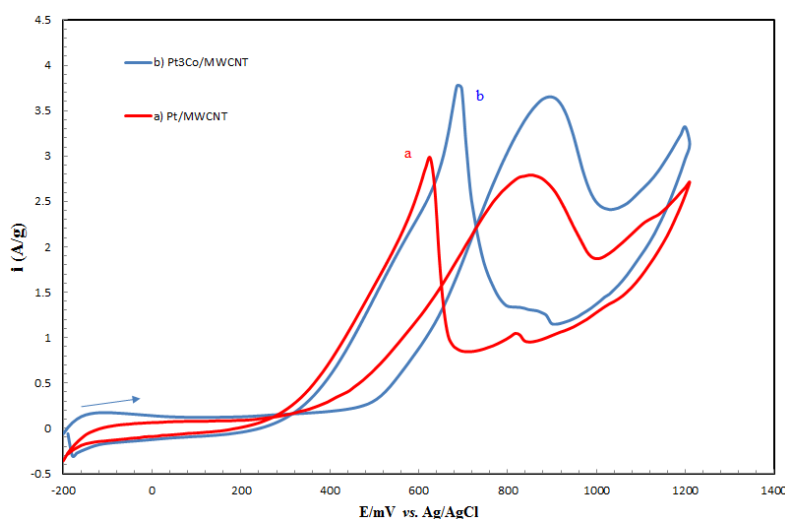
Fig. 5. The cyclic voltammograms of Pt/MWCNTs and Pt₃Co/MWCNTs electrocatalyst samples, in 0.5 M H₂SO₄ solution containing 1 M CH₃OH. The potential range is from −200 to +1200 mV at scan rate of 50 mV s⁻¹.

They remained due to MWCNTs' purification in mixed solution of nitric and sulfuric acids. They possibly regenerate Pt–CO_ads sites [48], as below:

$$CNT–OH + Pt–CO_{ads} \rightarrow CNT + Pt + CO_2 + H^+ + e^- \quad (5)$$

As CNTs defect, the dangling bonds may be simply oxidized at a low capacity to groups containing oxygen. Adding cobalt decreases the required potential for electrolysis of water, and as a result, the corresponding carbon oxidation [49, 50], as follows :

$$CNT+Pt–Co+H_2O \rightarrow CNT–OH+Pt–Co–H \quad (6)$$
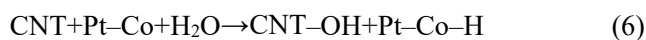
This limits the poisoning CO species' accumulation and produces numerous active sites for MOR. Generally, methanol concentration greatly affects the potential values of MOR and the current density. Therefore, Fig. 6 represents the cyclic voltammograms of Pt₃Co/MWCNTs electrocatalysts in 0.5 M H₂SO₄ solution exposed to various concentrations of methanol from 0.5 to 2 M. As the concentration of methanol rises, the values of oxidation current density rise at the first and the second peaks with a small potential change in the positive direction. More molecules of methanol are possibly adsorbed on the active sites of catalyst and enhance the obtained oxidation current density. In the backward direction, this enhances the current density of the associated reverse oxidation peak. Nevertheless, increased values of current density are recorded at Pt₃Co/MWCNTs electrocatalyst via addition of methanol until a concentration value of 1 M is obtained. This confirms the good electrocatalytic function of Pt₃Co/MWCNTs electrocatalyst versus the oxidation reaction of methanol.
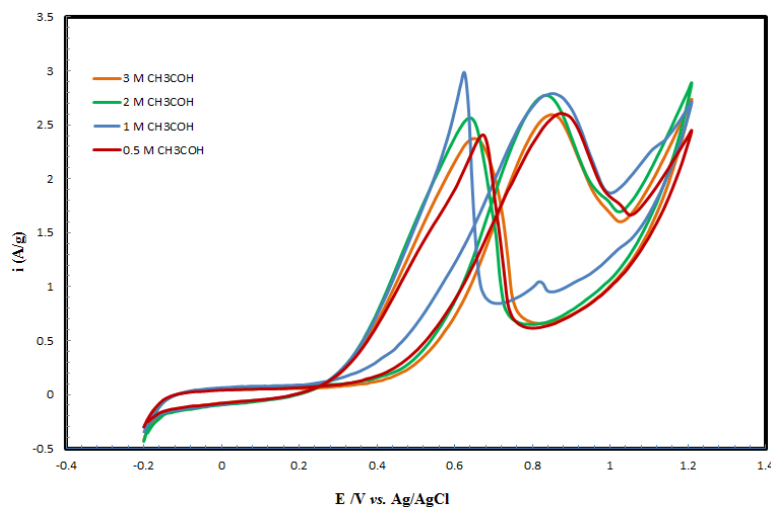

Fig. 6. The cyclic voltammograms of Pt₃Co/MWCNTs electrocatalysts, in 0.5 M H₂SO₄ solution containing 0.5, 1, 1.5, 2 M CH₃OH. The potential range is from −200 to +1200 mV at scan rate of 50 mV s⁻¹.

The lengthy electrocatalytic stabilities of the Pt₃Co/MWCNT catalyst were examined by chronoamperometry toward MOR at the 0.6 V potential. As can be seen from Fig. 7, the catalyst's current density declined quickly in the first stage, this is possibly attributed to the poisoning of catalyst through species of chemisorbed carbonaceous formed in MOR [51]. After a long period of time, the potentiostatic current decayed gradually, and a pseudo-steady condition was created. The Pt₃Co/MWCNT catalyst could maintain the largest current density all time, rendering the most favorable electrocatalytic function. This is in line with the cyclic voltammograms' behavior, not only assigned to the synergistic influence of the bimetallic active components, but also to the acceptable maintenance of the intrinsically electronic conductivity of MWCNTs.

3.3. Kinetic investigation of methanol electro-oxidation at Pt₃Co/MWCNT

The transportation properties of methanol on the Pt₃Co/MWCNT catalyst were studied through changing the rate of scanning; the associated voltammograms are depicted in Fig. 8a. The association between the square root of scan rate (v) and the forward peak current density (i_p) is shown in Fig. 8b. A linear relationship is detected,

suggesting that the forward peak potential E_P elevated with the scan rate (v); another linear relationship between E_P and long (v) was gained (Fig. 8c), showing that the methanol oxidation is an irreversible process [52-54]. Oxidation of methanol is handled by a process of diffusion on modified GCE of Pt₃Co/MWCNT. So, the greater coefficient of diffusion shows a useful impact on methanol oxidation kinetics.
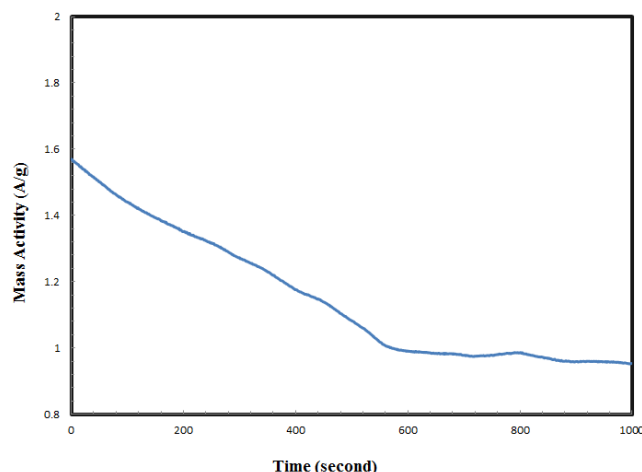

Fig. 7. The *i-t* curves of PtCo/MWCNT catalyst sample at 0.6 V for 1000 s in 0.5 M H_2SO_4 solution containing 1 M CH_3OH.
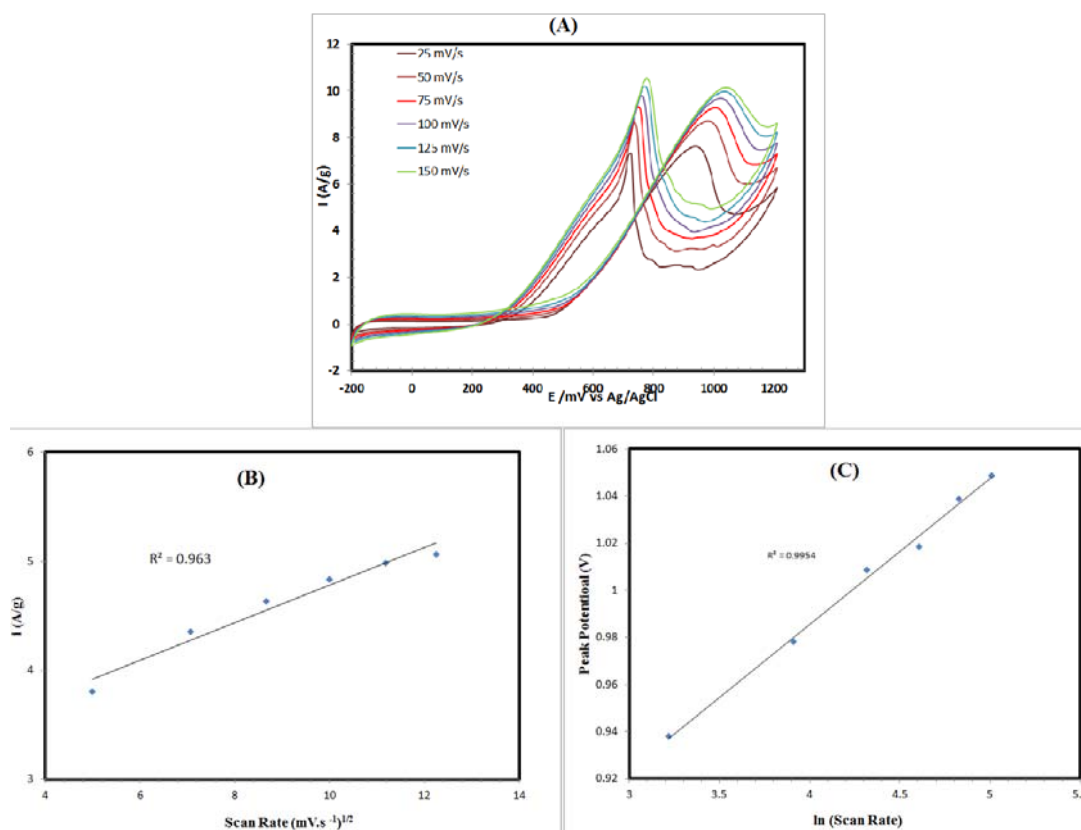

Fig. 8. (a) The cyclic voltammograms of Pt₃Co/MWCNTs electrocatalyst sample, in 0.5 M H_2SO_4 solution containing 1 M CH_3OH. Inner to outer; scan rate is 25, 50, 75, 100, 125 and 150 mVs⁻¹. (b) i_p *vs.* $v^{1/2}$ plot and (c) E_p *vs.* ln (v) plot.

4. Conclusions

Employing the impregnation method, Pt_3Co and Pt supported multi-walled carbon nanotubes were synthesized with $NaBH_4$. Cyclic voltammetry showed that the catalysts of Pt_3Co were active electrochemically in methanol oxidation and hydrogen adsorption/desorption. Based on the findings, the Pt_3Co/MWCNT catalyst with an acceptable alloying rate has better anti-poisoning ability, electrochemical activity, and long-term durability than catalysts of Pt/MWCNT, approved by the bimetallic catalysts' bi-functional mechanism. A great amount of Pt–Co pairs has the combination impact. Co site is used as an enhancing center for the production of Co–OH species, so more sites of Pt are accessible for oxidation of methanol. The results indicate that the higher Pt_3Co/MWCNT electrocatalytic activity and platinum active sites' stability in MOR can be attributed mainly to the composition of intermetallic Pt_3Co nanoparticles on MWCNTs. The fabrication procedure of Pt_3Co/MWCNT catalysts which makes the electro-oxidation of methanol easier possesses a paramount success in developing DMFCs.

Acknowledgements

References

[1] A. Arico, S. Srinivasan, V. Antonucci, Fuel Cells 1 (2001) 133-161.

[2] S. Basri, S.K. Kamarudin, W.R.W. Daud, Z. Yaakub, Int. J. Hydrogen Energy 35 (2010) 7957-7970.

[3] K.-Y. Chan, J. Ding, J. Ren, S. Cheng, K.Y. Tsang, J. Mater. Chem. 14 (2004) 505-516.

[4] L. Bai, H. Zhu, J.S. Thrasher, S.C. Street, ACS App. Mater. Interfaces 1 (2009) 2304-2311.

[5] C. Lamy, A. Lima, V. LeRhun, F. Delime, C. Coutanceau, J.-M. Léger, J. Power Sources 105 (2002) 283-296.

[6] B. Gurau, R. Viswanathan, R. Liu, T.J. Lafrenz, K.L. Ley, E. Smotkin, E. Reddington, A. Sapienza, B.C. Chan, T.E. Mallouk, J. Phys. Chem. B 102 (1998) 9997-10003.

[7] K.L. Ley, R. Liu, C. Pu, Q. Fan, N. Leyarovska, C. Segre, E. Smotkin, J. Electrochem. Soc. 144 (1997) 1543-1548.

[8] F. Alidusty, A. Nezamzadeh-Ejhieh, Int. J. Hydrogen Energy 41 (2016) 6288-6299.

[9] A. Ehsani, R. Asgari, A. Rostami-Vartooni, H.M. Shiri, A. Yeganeh-Faal, Iran. J. Catal. 6 (2016) 269-274.

[10] M.S. Tohidi, A. Nezamzadeh-Ejhieh, Int. J. Hydrogen Energy 41 (2016) 8881-8892.

[11] M.H. Sheikh-Mohseni, A. Nezamzadeh-Ejhieh, Electrochim. Acta, 147 (2014) 572-581.

[12] N.V. Long, M. Ohtaki, T.D. Hien, R. Jalem, M. Nogami, J. Nanopart. Res. 13 (2011) 5177.

[13] N.V. Long, Y. Yang, C.M. Thi, N. Van Minh, Y. Cao, M. Nogami, Nano Energy 2 (2013) 636-676.

[14] V. Bambagioni, C. Bianchini, A. Marchionni, J. Filippi, F. Vizza, J. Teddy, P. Serp, M. Zhiani, J. Power Sources 190 (2009) 241-251.

[15] T. Maiyalagan, Int. J. Hydrogen Energy 34 (2009) 2874-2879.

[16] T. Maiyalagan, J. Power Sources 179 (2008) 443-450.

[17] B. Rajesh, K.R. Thampi, J.-M. Bonard, N. Xanthapolous, H. Mathieu, B. Viswanathan, Electrochem. Solid State Lett. 5 (2002) E71-E74.

[18] H. Pang, J. Lu, J. Chen, C. Huang, B. Liu, X. Zhang, Electrochim. Acta 54 (2009) 2610-2615.

[19] H. Song, X. Qiu, F. Li, Electrochim. Acta 53 (2008) 3708-3713.

[20] H. Song, X. Qiu, F. Li, App. Catal. A 364 (2009) 1-7.

[21] Z. Liu, B. Guo, L. Hong, T.H. Lim, Electrochem. Commun. 8 (2006) 83-90.

[22] S. Song, J. Liu, J. Shi, H. Liu, V. Maragou, Y. Wang, P. Tsiakaras, App. Catal. B 103 (2011) 287-293.

[23] J. Zhao, P. Wang, W. Chen, R. Liu, X. Li, Q. Nie, J. Power Sources 160 (2006) 563-569.

[24] H. Huang, X. Wang, J. Mater. Chem. A 2 (2014) 6266-6291.

[25] S. Sharma, B.G. Pollet, J. Power Sources 208 (2012) 96-119.

[26] B. Stoner, B. Brown, J. Glass Diamond Relat. Mater. 42 (2014) 49.

[27] A. Bonesi, G. Garaventa, W. Triaca, A.C. Luna, Int. J. Hydrogen Energy 33 (2008) 3499-3501.

[28] W. Chen, J. Kim, S. Sun, S. Chen, Langmuir 23 (2007) 11303-11310.

[29] S. Koh, J. Leisch, M.F. Toney, P. Strasser, J. Phys. Chem. C 111 (2007) 3744-3752.

[30] D. Susac, A. Sode, L. Zhu, P. Wong, M. Teo, D. Bizzotto, K. Mitchell, R. Parsons, S. Campbell, J. Phys. Chem. B 110 (2006) 10762-10770.

[31] N. Atar, T. Eren, M.L. Yola, H. Karimi-Maleh, B. Demirdögen, RSC Adv. 5 (2015) 26402-26409.

[32] C.-T. Hsieh, J.-Y. Lin, J. Power Sources 188 (2009) 347-352.

[33] C.-T. Hsieh, J.-Y. Lin, J.-L. Wei, Int. J. Hydrogen Energy 34 (2009) 685-693.

[34] R. Amin, K. El-Khatib, R.A. Hameed, E.R. Souaya, M.A. Etman, App. Catal. A 407 (2011) 195-203.

[35] S. Aghdasi, M. Shokri, Iran. J. Catal. 6 (2016) 481-487.

[36] B. Khodadadi, M. Bordbar, Iran. J. Catal. 6 (2016) 37-42.

[37] L. Gao, L. Ding, L. Fan, Electrochim. Acta 106 (2013) 159-164.

[38] A. Nouralishahi, A.A. Khodadadi, Y. Mortazavi, A. Rashidi, M. Choolaei, Electrochim. Acta 147 (2014) 192-200.

[39] A. Kabbabi, R. Faure, R. Durand, B. Beden, F. Hahn, J.M. Leger, C. Lamy, J. Electroanal. Chem. 444 (1998) 41-53.

[40] R. Ahmadi, M. Amini, J. Bennett, J. Catal. 292 (2012) 81-89.

[41] R. Crisafulli, R. Antoniassi, A.O. Neto, E. Spinacé, Int. J. Hydrogen Energy 39 (2014) 5671-5677.

[42] E. Antolini, J.R. Salgado, E.R. Gonzalez, App. Catal. B 63 (2006) 137-149.

[43] J. Zhao, A. Manthiram, App. Catal. B 101 (2011) 660-668.

[44] J.G. de la Fuente, S. Rojas, M. Martínez-Huerta, P. Terreros, M. Pena, J. Fierro, Carbon 44 (2006) 1919-1929.

[45] E. Lust, E. Härk, J. Nerut, K. Vaarmets, Electrochim. Acta 101 (2013) 130-141.

[46] M.M. Mohamed, M. Khairy, S. Eid, J. Power Sources 304 (2016) 255-265.

[47] M.M. Mohamed, S. Eid, A. El-Etre, J. Photochem. Photobio. A 338 (2017) 37-48.

[48] J. Chen, M. Wang, B. Liu, Z. Fan, K. Cui, Y. Kuang, J. Phys. Chem. B 110 (2006) 11775-11779.

[49] Y. Lin, X. Cui, C.H. Yen, C.M. Wai, Langmuir 21 (2005) 11474-11479.

[50] Y. Wang, J. Clancey, G. Lu, J. Liu, L. Liu, J. Chaudhuri, S. George, M. Xie, S. Wei, Z. Guo, J. Electrochem. Soc. 163 (2016) F1-F10.

[51] Y. Li, L. Tang, J. Li, Electrochem. Commun. 11 (2009) 846-849.

[52] W. Ye, Y. Chen, Y. Zhou, J. Fu, W. Wu, D. Gao, F. Zhou, C. Wang, D. Xue, Electrochim. Acta 142 (2014) 18-24.

[53] W. Ye, H. Hu, H. Zhang, F. Zhou, W. Liu, App. Surf. Sci. 256 (2010) 6723-6728.

[54] H. Tong, H.-L. Li, X.-G. Zhang, Carbon 45 (2007) 2424-2432.